Anal Bioanal Chem (2012) 404:3025–3036
DOI 10.1007/s00216-012-6417-5

ORIGINAL PAPER

The in vivo biodistribution and fate of CdSe quantum dots in the murine model: a laser ablation inductively coupled plasma mass spectrometry study

TsingHai Wang · HuiAn Hsieh · YiKong Hsieh · ChiShiun Chiang · YuhChang Sun · ChuFang Wang

Received: 15 July 2012 / Revised: 29 August 2012 / Accepted: 6 September 2012 / Published online: 7 October 2012

Abstract Understanding the cytotoxicity of quantum dots strongly relies upon the development of new analytical techniques to gather information about various aspects of the system. In this study, we demonstrate the in vivo biodistribution and fate of CdSe quantum dots in the murine model by means of laser ablation inductively coupled plasma mass spectrometry (LA-ICP-MS). By comparing the hot zones of each element acquired from LA-ICP-MS with those in fluorescence images, together with hematoxylin and eosin-stained images, we are able to perceive the fate and in vivo interactions between quantum dots and rat tissues. One hour after intravenous injection, we found that all of the quantum dots had been concentrated inside the spleen, liver and kidneys, while no quantum dots were found in other tissues (i.e., muscle, brain, lung, etc.). In the spleen, cadmium-114 signals always appeared in conjunction with iron signals, indicating that the quantum dots had been filtered from main vessels and then accumulated inside splenic red pulp. In the liver, the overlapped hot zones of quantum dots and those of phosphorus, copper, and zinc showed that these quantum dots have been retained inside hepatic cells. Importantly, it was noted that in the kidneys, quantum dots went into the cortical areas of adrenal glands. At the same time, hot zones of copper appeared in proximal tubules of the cortex. This could be a sign that the uptake of quantum dots initiates certain immune responses. Interestingly, the intensity of the selenium signals was not proportional to that of cadmium in all tissues. This could be the result of the decomposition of the quantum dots or matrix interference. In conclusion, the advantage in spatial resolution of LA-ICP-MS is one of the most powerful tools to probe the fate, interactions and biodistribution of quantum dots in vivo.

Keywords Laser ablation inductively coupled plasma mass spectrometry · Quantum dots · Biodistribution · Fate of quantum dots · In vivo

Introduction

Quantum dots (QDs) are crystalline semiconductor nanoparticles with diameters of a few nanometers. Their extremely small size along with the consequential quantum confinement effect allow for a wide range of application including as solar energy harvest [1–4], optoelectronics [5–7], and biomedicine [8–11]. In the regime of biomedical applications, researchers work on focusing both diagnostic (e.g., imaging probes) and therapeutic (e.g., drug delivery vehicles) related studies [12]. Despite the fact that more and more cutting edge quantum dots have been synthesized, two essential puzzles remain unclear and must be solved: their cytotoxicity and in vivo interactions.

The main concern, cytotoxicity of quantum dots, stems from two properties: their heavy metal content (such as Cd, Se, and Te) and their high surface activity (due to their extremely small sizes). Related literature reports severe

Electronic supplementary material The online version of this article (doi:10.1007/s00216-012-6417-5) contains supplementary material, which is available to authorized users.

T. Wang · C. Chiang · C. Wang
Institute of Nuclear Engineering and Sciences,
National Tsing Hua University,
Hsinchu City 30012, Taiwan

H. Hsieh · Y. Hsieh · C. Chiang · Y. Sun · C. Wang (✉)
Department of Biomedical Engineering and Environmental Sciences, National Tsing Hua University,
Hsinchu City 30012, Taiwan
e-mail: cfwang@mx.nthu.edu.tw

discrepancies as to whether quantum dots are cytotoxic. On one hand, it was reported that CdSe quantum dots show acute toxicity toward hepatocytes. Their cytotoxicity comes from the released cadmium due to decomposition of quantum dots. To slow down the degradation rate and therefore reduce toxicity, one effective solution is to pay special attention to the synthesis of the quantum dots. Several factors, including the synthesis routes, exposure time to ultraviolet light, and a thin inert outer layer, dramatically impact on the toxicity of as-acquired quantum dots [13]. Alternatively, one may argue that all above-mentioned experiments were conducted adopting the "proof-of-principle" approach. That is, experiments were conducted using an extremely high concentration of quantum dots. Such compromised experiment design is beneficial in the restriction of analytical instruments used but is obviously far from the physiological conditions. From a scientific perspective, the proposed cytotoxicity may be exaggerated [14].

Correcting this discrepancy strongly relies on the progress of analytical approaches. To date, state-of-the-art analytical tools that might be able to fulfill these requirements we mentioned above include fluorescence imaging techniques [15, 16], positron emission tomography [17, 18], secondary ion mass spectroscopy (SIMS) [19–21], and inductively coupled plasma mass spectroscopy (ICP-MS) [22]. Also, some interesting reports regarding the interaction between gold nanoparticles and cells were found using laser desorption/ionization mass spectrometry [23, 24].

Despite many successful achievements have been done in surface analysis, application of SIMS toward bio samples is quite limited since most bio samples are unstable in a vacuum system. Fluorescence imaging techniques have very high sensitivity toward quantum dots, but suffer matrix effects that absorb or interfere with the emission of fluorescence. As a result, a thinner slice sample is much more suitable for fluorescence image analysis. Positron emission tomography is advantageous because it is a non-invasion technique. Its spatial resolution, however, is strongly restricted by the intrinsic property that the detection of high-energy photons is very poor. Inductively coupled plasma mass spectroscopy is well known for its extremely low detection limit for most elements, particularly the part-per-billion level for most transition metals. However, samples need to be digested or dispersed into liquid unless additional components, such as a tandem laser ablation system, are connected to the detection component.

In this study, we explored the fate and the biodistribution of CdSe quantum dots in rat tissues by means of laser ablation inductively coupled plasma mass spectrometry (LA-ICP-MS). The laser ablation component evaporates a localized area of the sample and introduces it into the ICP-MS component for qualitative analysis. By scanning the entire sample, the spatial distribution of quantum dots is observed. Together with hematoxylin and eosin (H&E) stained image, we can observe the histological positions where these quantum dots locate to study their biointeractions. With these comprehensive analysis results, we are able to estimate the possible cytotoxicity of quantum dots in vivo.

Theory

Evaluating the cytotoxicity of quantum dots involves the solution of two fundamental challenges: where these quantum dots locate (biodistribution) and how they interact with surrounding cells. To probe the location of quantum dots, an analytical instrument should possess high sensitivity and low detection limits. For these reasons, mass spectroscopy is one of the most suitable analytical instruments for such tasks. Inductively coupled plasma mass spectrometry is well known its high sensitivity toward most metal ions, and it is capable of multielement analysis at the same time. The latter property makes mass spectroscopy more practical than fluorescence spectroscopy as the abnormal distribution of some essential elements is usually a sign of disease or immune reactions to stimuli. Mass spectrometry can be performed to determine the amounts of many elements at the same time, while fluorescence spectroscopy can only be used to analyze the components that fluoresce. For example, the inactivation of Cu-ATPase induced by either Wilson disease or Menkes disease results in an abnormal copper accumulation in the kidneys [25]. Despite two such advantages, mass spectroscopy alone is not capable of probing the biointeractions between quantum dots and surrounding cells. A new sample introduction component to a mass spectrometer that avoids conventional pretreatment procedures such as dissolution and digestion is necessary. The use of a laser ablation system is proposed to directly evaporate solid samples and then introduce them into the analytical component. When operating in scanning mode, the laser scans solid samples pixel by pixel, and an image containing multielement information within each grid is acquired. Equipping both a low-detection limit and the capability of two-dimensional image acquisition, LA-ICP-MS is able to acquire the spatial distributions of elements of interest with lateral and depth resolution in micrometer scale [26].

Experimental section

CdSe quantum dots

The quantum dots used in this study were purchased from Invitrogen (Hayward, CA, USA) as Qdot® 705 ITKTM carboxyl quantum dot. Their average particle size is about 13 nm with a mean molecular weight of approximately

1.5 MDa. They were used as received without further treatments.

Laser ablation inductively coupled plasma mass spectrometry

Laser ablation was performed using a UP 213 laser ablation system (New Wave Research, USA) utilizing a Nd:YAG laser with wavelength of 213 nm and operated in Q-switched (Pulsed) mode. The pulse length is 4 ns with repetition rate of 10 Hz with a dwell time of 8 s and an intersite pause of 1 s. During ablation, the laser beam (diameter, 0.11 mm; defocused distance, 1.5 mm) with fluence of 15–20 Jcm^{-2} was used to vaporize the elements in a selected area. With 0.1 mm/s of scan speed and frequency of 10 Hz, an area about 10 mm × 10 mm (depending on the actual size of the sample) was ablated and introduced into ICP-MS using argon as the carrier gas (1.0 L/min). Multielement analysis was conducted using a quadrupole ICP mass spectrometer (Agilent 7500a, USA). The operation RF power was 1.5 kW using the detector in time-resolved analysis acquisition mode. Plasma gas flow rate and auxiliary gas flow rate were 15 and 2.0 L/min, respectively.

Fluorescence microscopy system

Fluorescence microscopy images of tissue sections and bright field microscopy images of H&E stained tissue sections were obtained by using an inverted fluorescence microscope (IX71, Olympus, Tokyo, Japan) equipped with a color CCD camera (DP72, Olympus, Tokyo, Japan). The sliced samples were photoexcited with irradiation of wavelength of 425 nm (the corresponding fluorescence emission is 710 nm). Since as-obtained fluorescence image was recorded directly by the CCD camera without any further image processing, the location of quantum dots was designated as the regions with bright green-yellowish (mustard color) whereas the places showing dark green mean there are no significant amount of quantum dots presented.

In vivo animal intravenous injection and sample collection

Four mice, around 6 weeks of age, were purchased from BioLASCO (Taipei, Taiwan). When they matured to ~200 g in weight, a suspension of CdSe quantum dots was injected intravenously into their jugular vein at a dose of 200 pmol/kg. They were killed 1 h after administration. Their brain, lung, muscle, liver, kidney, and spleen were collected following the procedure reported in literature [12]. These samples were immediately embedded into Optimal Cutting Temperature Compound and then frozen down to −20 °C. These frozen samples were sliced by a freezing microtome with thickness of 20 μm. As-prepared samples were mounted on silane-coated slides (Muto Pure Chemicals Co. Ltd., Tokyo, Japan) and then stored in −20 °C before analysis. For histological studies, part of these samples were stained with hematoxylin and eosin (H&E) and observed by an optical microscope. For comparison, fluorescence microscopy images were taken first. Identical samples were consequentially analyzed by LA-ICP-MS and selected essential elements including ^{31}P, ^{56}Fe, ^{57}Fe, ^{63}Cu, ^{66}Zn, ^{82}Se, and ^{114}Cd were monitored.

Image composition and statistical analysis

In order to compose the pixel-by-pixel information acquired from LA-ICP-MS, a home-built image-processing code based on the Matlab interface was used. The intensity of these elements was converted into an 8-bit color image with variable darkness. A map with the spatial distribution of each element was thus obtained. For statistical analysis, the correlation coefficient between each element was automatically generated by our code based on Eq. (1)

$$r_{xy} = \frac{\sum_i x_i y_i - \frac{1}{n}\sum x_i \sum y_i}{\sqrt{\sum_i (x_i - \bar{x})^2}\sqrt{\sum_i (y_i - \bar{y})^2}} \quad (1)$$

where x_i and y_i are the element we monitored, $\bar{x}$ and $\bar{y}$ are the average intensity (counts) of these elements and r is the correlation coefficient.

Results and discussion

It should first be pointed out that while there were only four mice studied, the distribution of quantum dots in each sample is very similar to the others. We are, therefore, confidently reporting the representative images herein. The presence of quantum dots was imaged using thin slides of tissues of the muscles, brain, lung, spleen, liver, and kidney. Quantum dots were found in the tissues of the spleen, liver, and kidneys, however no quantum dots were found elsewhere (muscle, lung, and brain). We also digested parts of muscle and brain samples for conventional ICP-MS analysis and no significant amount of Cd was found. Such solid evidence clearly pointed out that no quantum dots were presented in these tissues. Reported results were observed using a combination of LA-ICP-MS and fluorescence microscopy. These observations indicate that despite injection of the quantum dots intravenously which allowed the quantum dots to travel throughout the entire body along with the blood, only these metabolism relevant organs interact with quantum dots. Similar observations have been reported as well with silica and diamond nanoparticles being found to accumulate in the spleen and liver [12, 18]. In addition, we present the correlation coefficient for each element that was monitored. Considering the inevitable interference resulting

from background matrix and the low intensity due to the dilution effect, we will avoid any quantitative interpretations on the basis of statistics results. Instead, we will present the correlations between quantum dots and each essential nutrient (^{31}P, ^{63}Cu, and ^{66}Zn) that was monitored.

The fate and interactions of quantum dots CdSe in the spleen

The spleen is the largest lymphatic organ and plays a very important role in the immune system. It consists of two histological components, the red pulp (~75 %) and the white pulp (~25 %). Red pulp is made up of cords of Billroth, or connective tissue, and many other splenic sinews that are engorged with blood, giving them a red color. The primary function of red pulp is to filter antigens, microorganisms, and defective or worn-out red blood cells from the bloodstream. Unlike red pulp, the white pulp contains lymphocytes such as T cells and B cells. Interactions between foreign objects with T cells and B cells are very important mechanisms of immune reactions.

The examined spleen samples were transverse sections that were sliced across the blood vessels (artery and vein) in the spleen. From our LA-ICP-MS results (Fig. 1a), there were several intense ^{114}Cd hot zones concentrated in the middle part of the spleen. By magnifying these hot zones (Fig. 1b), it became evident that the quantum dots were concentrated as clusters or islands separated by voids in which no quantum dots were spotted. Based on this evidence, the quantum dots are taken up distributed inhomogeneously in the spleen. These results also emphasize the importance of using an appropriate sample introduction system such as laser ablation system. If we adopted a conventional sample introduction system, which requires samples to be digested and then dispersed into a solution matrix, we would have observed the average quantum dot concentration without any data related to the in vivo distribution of the quantum dots. Fig. 1d is the corresponding fluorescence image showing the identical magnification and region as that in Fig. 1b. In this fluorescence image, regions in yellow reflect the fluorescence emission from quantum dots, whereas those in the dark green represent areas without quantum dots. Comparison of Fig. 1b and d clearly indicate that the observed ^{114}Cd originates from the intact quantum dots since the degraded or compromised quantum dots will not fluoresce. Such comparison demonstrates that LA-ICP-MS and fluorescence spectra are complementary techniques to probe the intactness of quantum dots. Taking H&E images (Fig. 1c) into consideration, it is evident that those dark green spots (Fig. 1d) and hot zones (Fig. 1b) are the areas where red pulp exists in the spleen. In brief, we realize that 1 h after intravenous injection, quantum dots will accumulate in the red pulp of the spleen and there is no evidence regarding the degradation of quantum dots that have been taken up. Our results are in a good agreement with those reported from Vachet and Rotello group, where they pointed out that no significant decomposition of quantum dots taking place within 5 h after administration [27].

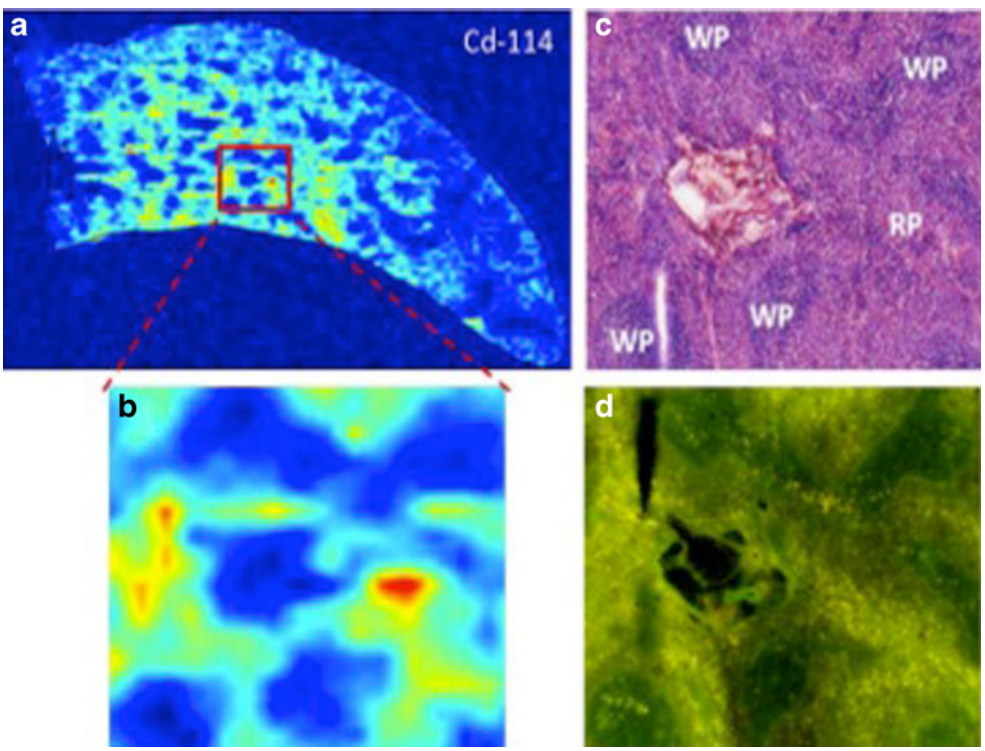

Fig. 1 **a** The Cd-114 mapping image in the spleen from LA-ICP-MS; **b** higher magnification of selected Cd-114 hot zone and **c** its corresponding H&E stained image, and **d** fluorescence image, the region with *red color* is the location of high intensity while the one in *blue* means very low intensity

Another impressed feature of LA-ICP-MS is its capability of concurrent multielement analysis (Fig. 2). Unfortunately, the low intensity of the peaks for ^{82}Se makes it difficult to extract from the background. Such result could easily lead to the conclusion of the decomposition of quantum dots. The low ^{82}Se intensity also results in poor r values for each element that was monitored (Table 1). From a statistical point of view, these results imply that the quantum dots begin decomposing within 1 h and the observed ^{114}Cd came from the released cadmium ions. The release of cadmium ions from quantum dots is a serious concern. In a recent study, a small-scale soil column experiment with 15 days of incubation was performed. The results showed that some degradation and/or surface modification of quantum dots CdSe has been observed. In this case, a chelating agent is the critical factor which affects the degree of degradation [28]. Also, it has been reported that over a period of 24 h, the stability of quantum dots decreases as the particle size increases [19]. Based on literature findings, it is likely that quantum dots are rather stable and significant degradation

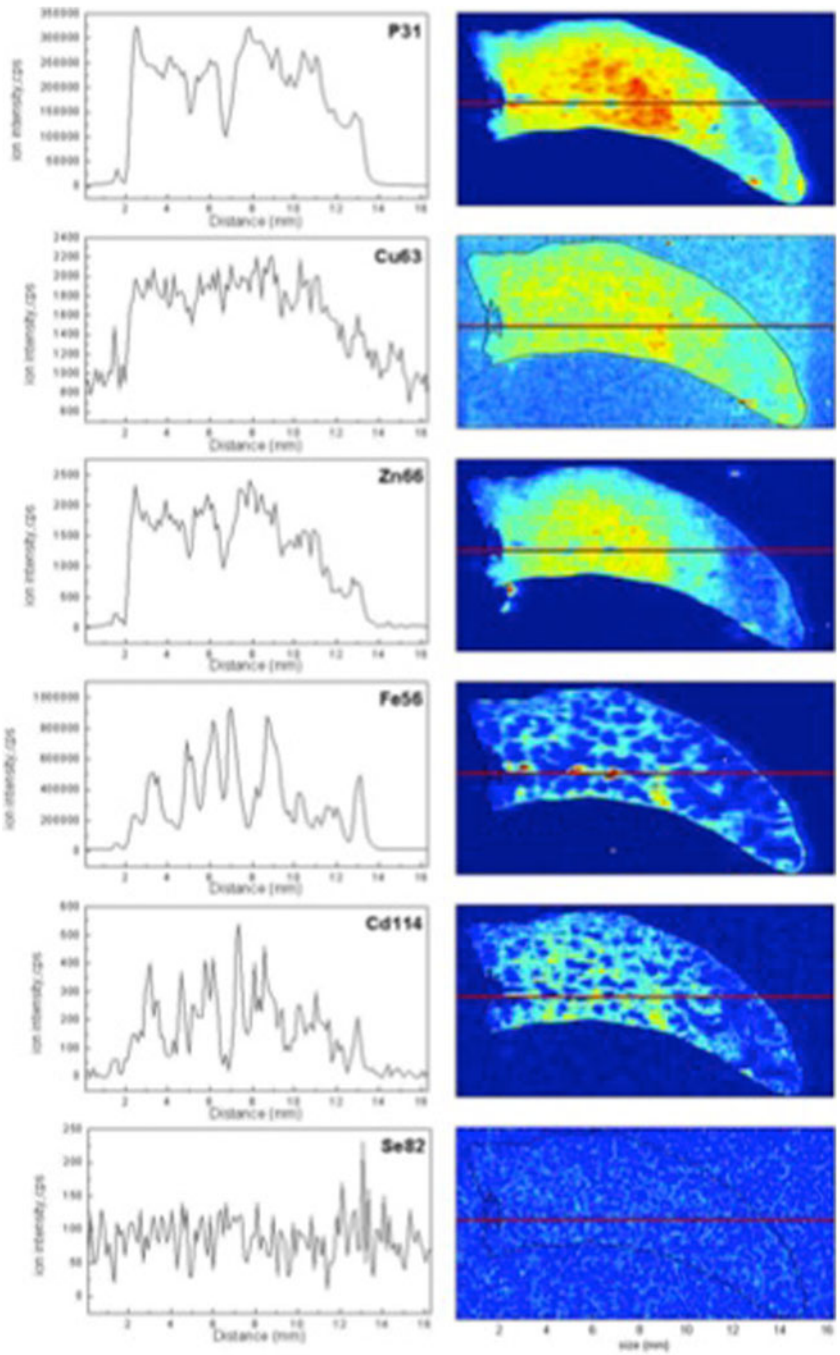

Fig. 2 The intensity profiles of each element (from top to bottom, ^{31}P, ^{63}Cu, ^{66}Zn, ^{56}Fe, ^{114}Cd, and ^{82}Se) in the spleen and their corresponding mapping images. Recorded intensity profiles were scanned along the indicated *red lines*, the region with *red color* is the location of high intensity while the one in *blue* means very low intensity. The *y*-axis shown in the right figures is the arbitrary unit showing counts per second the LA-ICP-MS read while the *x*-axis is the distance samples were scanned (mm). See Fig S1 of the Electronic supplementary material for the distribution of ^{31}P, ^{63}Cu, and ^{66}Zn, in the spleen of control experiments

Table 1 The correlation between each monitored elements in the spleen

r	P-31	Cu-63	Zn-66	Fe-56	Cd-114	Se-82
P-31	1					
Cu-63	0.8107	1				
Zn-66	0.9232	0.8448	1			
Fe-56	0.4525	0.6619	0.5593	1		
Cd-114	0.5198	0.7057	0.5945	0.7076	1	
Se-82	0.0392	0.0145	0.0540	0.0725	0.0540	1

does not occur in 24 h even when chelating agents are presence. As a result, the low ^{82}Se intensity should be interpreted as a consequence of matrix interference and relatively low detection sensitivity (compared to cadmium). Considering the huge dilution effect from blood circulation, there must be a significant number of intact quantum dots accumulating in the red pulp or we would not observe the intense fluorescence in Fig. 1d.

Putting aside the dispute over whether quantum dots are compromised, there were additional features that were observed using LA-ICP-MS. First, the intensity profile of ^{114}Cd resembles that of ^{56}Fe very much. There is a high concentration of iron in red blood cells which are present in the red pulp of the spleen. Based on these observations, presented in Fig. 1, the quantum dots are particularly accumulated in red pulp that is full of blood. Secondly, the intensity profiles of ^{31}P, ^{63}Cu, and ^{66}Zn are comparable with one another, spreading homogeneously throughout the spleen. This interesting observation indicates that the distribution of these essential elements is not affected by foreign quantum dots. Lastly, no significant amount of quantum dots was found in places without ^{56}Fe. From these results, together with results from fluorescence and H&E stained images, it is evident that no quantum dots appear in the white pulp of the spleen. This is very important because if quantum dots are recognized as "bad" objects, due to their comparable size to many microorganisms, they should trigger immune reactions and then be attacked by both T cells and B cells in white pulps. Whether or not T cells and B cells are capable of attacking these quantum dots, we should be able to spot ^{114}Cd inside white pulps. These observations suggest that quantum dots do not initiate any acute immune responses in the spleen.

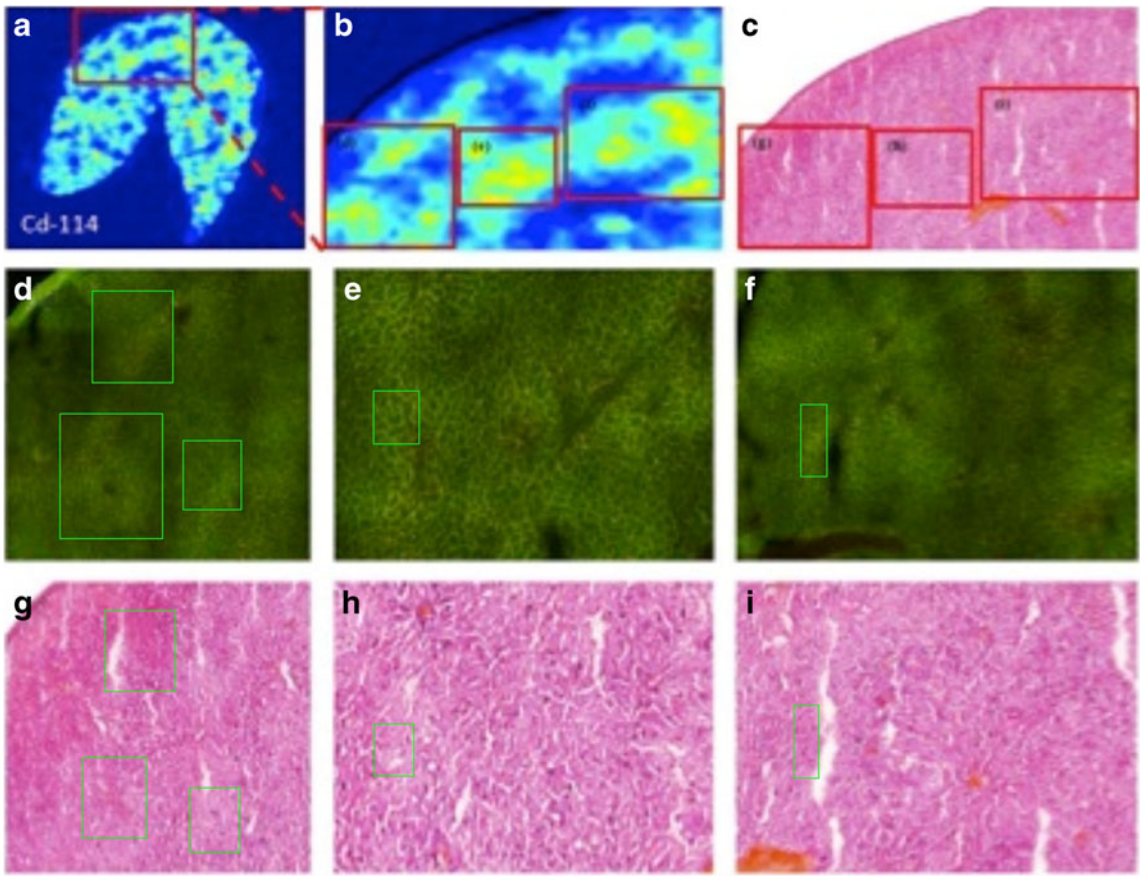

Fig. 3 **a** The ^{114}Cd mapping image in liver from LA-ICP-MS; **b** higher magnification of selected ^{114}Cd hot zone as shown in (**a**); and its corresponding H&E stained image (**c**); fluorescence images of selected area (**d**–**f**), and their corresponding H&E stained image (**g**–**i**), the region with *red color* is the location of high intensity while the one in *blue* means very low intensity

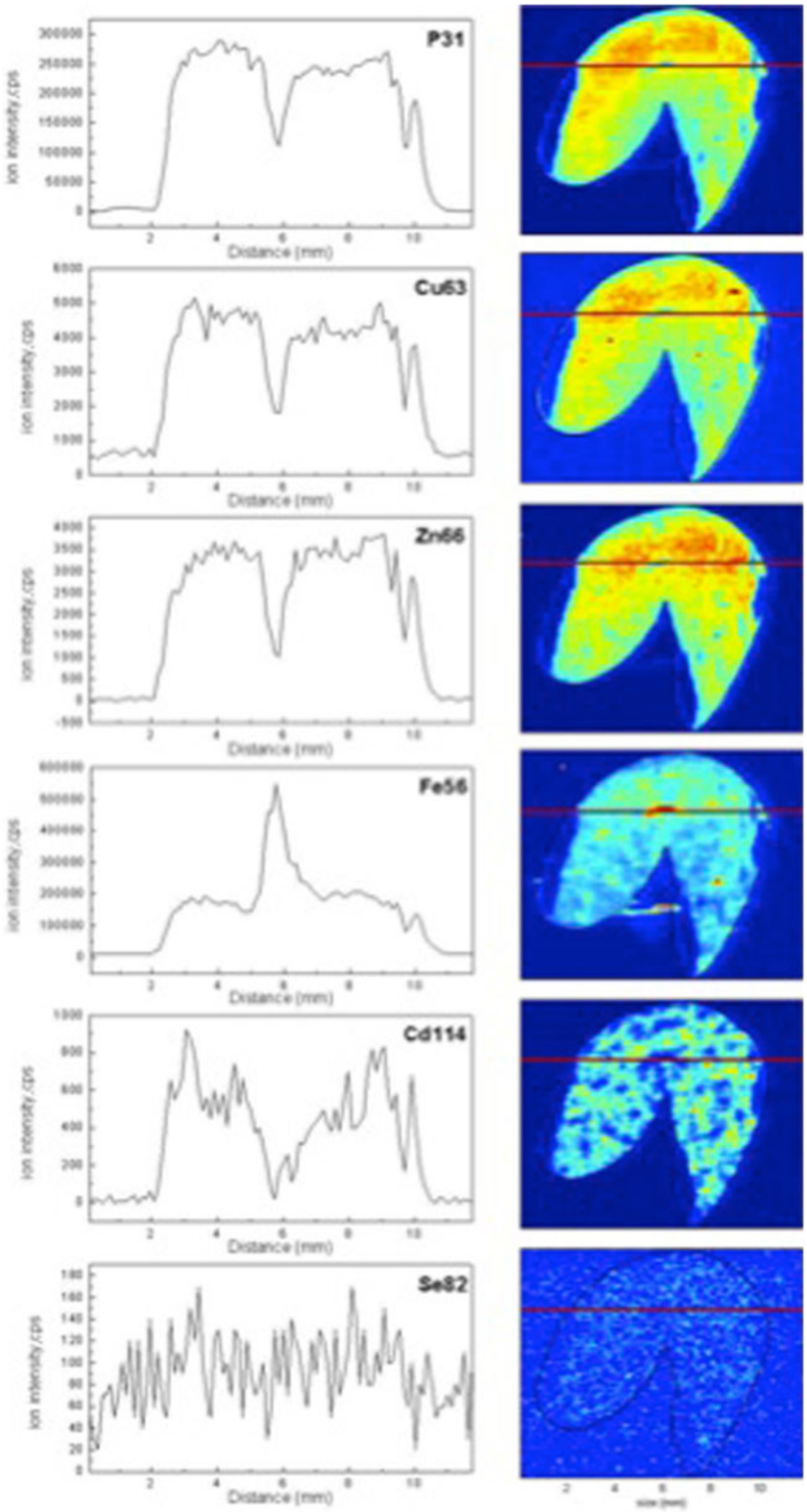

Fig. 4 The intensity profiles of each element (*from top to bottom*, ^{31}P, ^{63}Cu, ^{66}Zn, ^{56}Fe, ^{114}Cd, and ^{82}Se) in the liver and their corresponding mapping images. Recorded intensity profiles were scanned along the indicated *red lines*, the region with *red color* is the location of high intensity while the one in *blue* means very low intensity. The *y*-axis shown in the right figures is the arbitrary unit showing counts per second the LA-ICP-MS read while the *x*-axis is the distance samples were scanned (mm). See Fig. S1 of the Electronic supplementary material for the distribution of ^{31}P, ^{63}Cu, and ^{66}Zn, in the liver of control experiments

The fate and interactions of quantum dots CdSe in the liver

The liver is a very important organ that is involved in many essential functions including protein synthesis, protein storage, transformation of carbohydrates, synthesis of cholesterol, bile salts and phospholipids, detoxification, modification and excretion of exogenous and endogenous substances. The main component in the liver is hepatocyte tissue, which makes up 75+% of the liver's cytoplasmic mass. These

Table 2 The correlation between each monitored element in the liver

r	P-31	Cu-63	Zn-66	Fe-56	Cd-114	Se-82
P-31	1					
Cu-63	0.9698	1				
Zn-66	0.9440	0.9452	1			
Fe-56	0.7146	0.6800	0.6878	1		
Cd-114	0.6654	0.6993	0.7242	0.3251	1	
Se-82	0.2865	0.2969	0.3046	0.1749	0.3043	1

laminal hepatocytes are separated by hepatic sinusoids (a kind of sinusoidal blood vessel). Blood coming from the hepatic artery will flow into the sinusoids, through the hepatic (centrilobilar) venules and finally drains out of the liver via the hepatic vein. In the portal circulation, a string of biochemical reactions take place which convert nutrients for usage or storage, and removing toxins at the same time.

From Fig. 3a, it was noted that, similar to the spleen, quantum dots were concentrated in certain region of the liver. With higher magnification (Fig. 3 d–i), it appears that the hot zones of ^{114}Cd situate in the portal area where the hepatic portal vein and hepatic artery exist (both hepatic portal veins and hepatic arteries locate look dark red in the image since they were full of blood. We drew several rectangular boxes as representatives to indicate where they are). From LA-ICP-MS (Fig. 4), we noticed that no ^{114}Cd was observed inside the blood vessel (the valley of ^{114}Cd corresponds to the summit of ^{56}Fe). Restricted by the spatial resolution of laser ablation (spot size of 0.11 mm in diameter), it is difficult to determine whether or not quantum dots have diffused through the main blood vessel. However, the intensity of ^{114}Cd increases concurrently with the decrease of ^{56}Fe, implying that the cadmium is not located in the blood vessels but is sequestered in the liver tissues. Furthermore, the intensity profile of ^{56}Fe is opposite to that of each of the essential metals (^{31}P, ^{63}Cu, and ^{66}Zn) that were monitored. The summit in the profile of ^{56}Fe coincides with the valleys in the profiles of the rest of the elements (Fig. 4). This is due to the essential elements residing in liver tissue itself, not in the blood vessels. Finally, similar to what we have observed in the spleen, signals of ^{82}Se are still ambiguous and difficult to distinguish from background noises. This explains the poor r value shown in Table 2. Despite the low intensity of ^{82}Se, however, we prefer to interpret that these quantum dots appear intact, since we observed the bright-yellow fluorescence in Fig. 3d–f.

The fate and interactions of quantum dots CdSe in the kidney

The kidneys are the essential organ of the urinary system which removes toxins and others wastes out of the bloodstream. It is composed of the outer cortex and the inner medulla. The most basic unit of the kidney is the nephron, which is made up of a renal corpuscle and its tubules. The renal corpuscle consists of the glomerulus and Bowman's

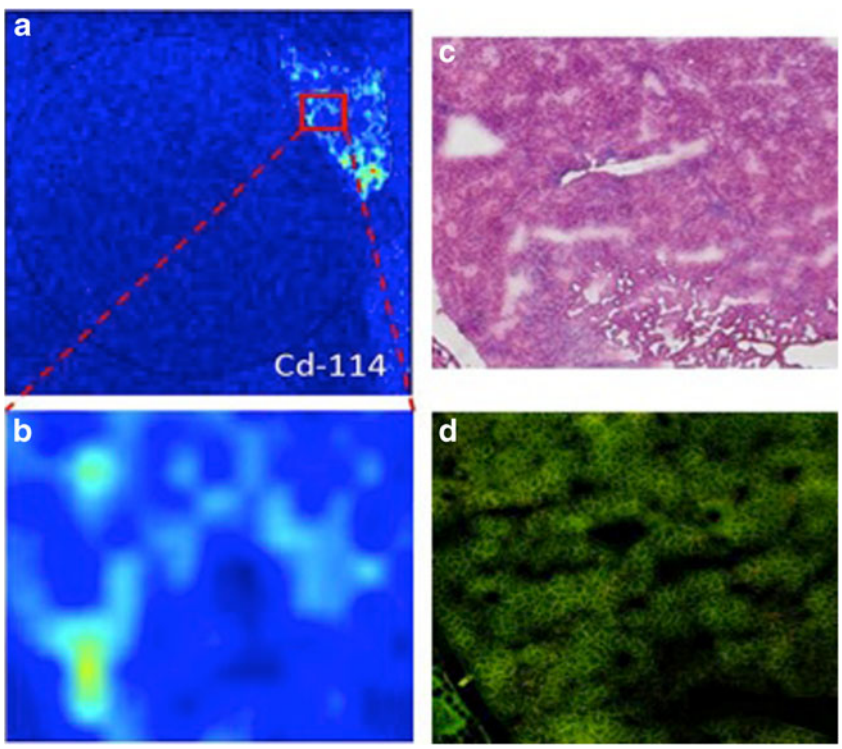

Fig. 5 **a** The ^{114}Cd mapping image in the kidney from LA-ICP-MS; **b** higher magnification of selected ^{114}Cd hot zone as shown in (**a**); and its corresponding H&E stained image (**c**); fluorescence images of selected area (**d**); the region with *red color* is the location of high intensity while the one in *blue* means very low intensity

capsule. These two components filter toxics and wastes out of blood. Based on this physiology, it is reasonably expected that quantum dots that have been filtered out of the blood would accumulate inside these renal corpuscles. Surprisingly, there was not any significant amount of ^{114}Cd around renal corpuscles (Fig. 6). Instead, several very intense ^{114}Cd hot zones appeared in adrenal gland (Fig. 5b–d). Additionally, the intensity profile of ^{114}Cd is rather asymmetric and quite different

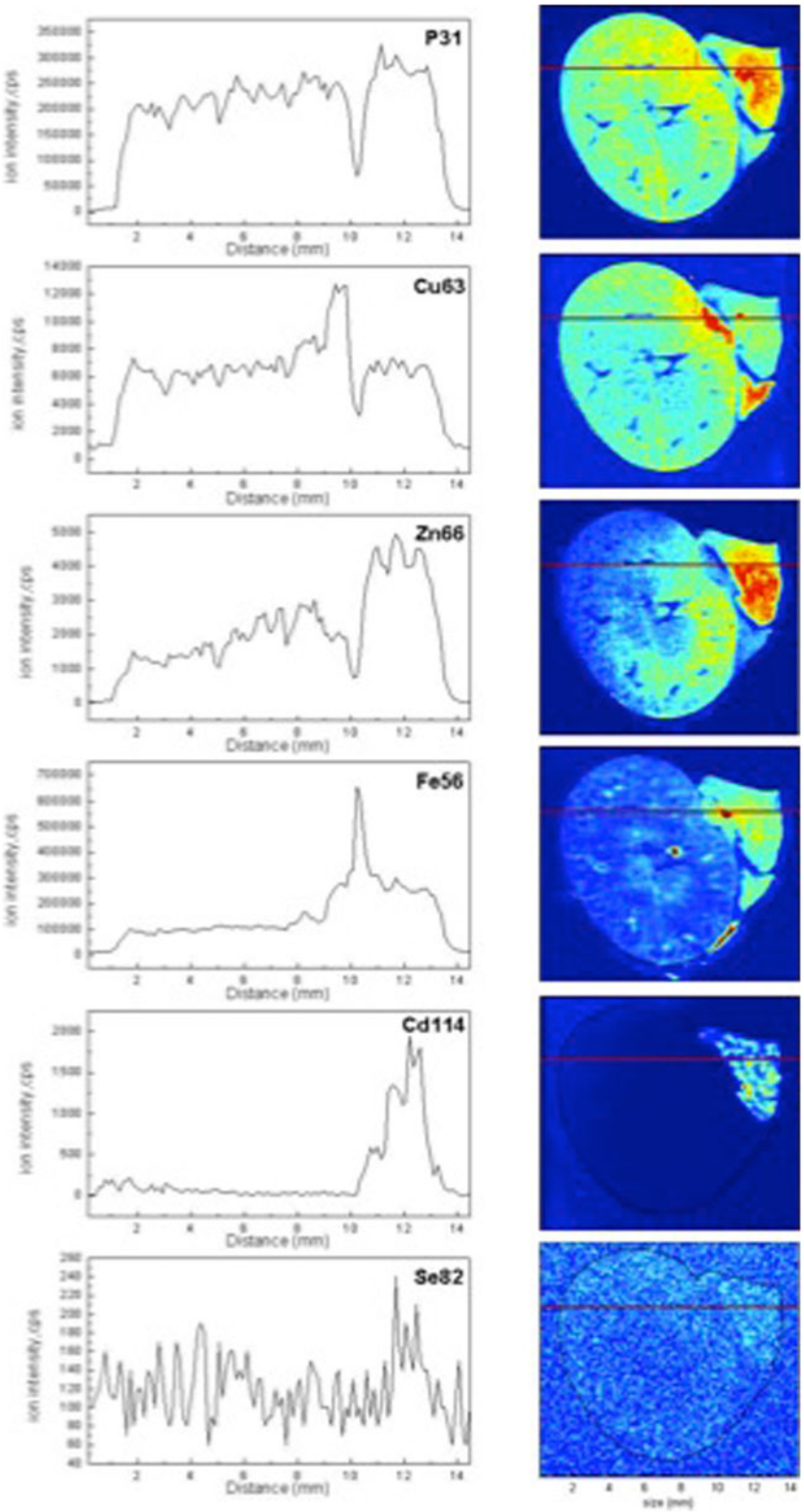

Fig. 6 The intensity profiles of each element (from top to bottom, ^{31}P, ^{63}Cu, ^{66}Zn, ^{56}Fe, ^{114}Cd, and ^{82}Se) in the kidney and their corresponding mapping images. Recorded intensity profiles were scanned along the indicated *red lines*; the region with *red color* is the location of high intensity while the one in *blue* means very low intensity. The *y*-axis shown in the right figures is the arbitrary unit showing counts per second the LA-ICP-MS read while the *x*-axis is the distance samples were scanned (mm)

Table 3 The correlation between each monitored elements in the kidney

r	P-31	Cu-63	Zn-66	Fe-56	Cd-114	Se-82
P-31	1					
Cu-63	0.9406	1				
Zn-66	0.9455	0.9191	1			
Fe-56	0.8532	0.8681	0.8130	1		
Cd-114	0.6908	0.5708	0.8055	0.5785	1	
Se-82	0.6731	0.7054	0.6597	0.6576	0.5599	1

from its patterns in the spleen and liver (Figs. 2 and 4). Similar to the results for the liver, no ^{114}Cd resided inside blood vessel as indicated by the concurrent summit of the ^{56}Fe intensity profile and valley of the ^{114}Cd intensity profile (Fig. 6). Based upon results from the spleen, liver and kidney, it is evident that quantum dots are filtered out of the bloodstream within 1 h. Again, the coexistence of blurry ^{82}Se signals and intensely bright-yellow fluorescence were observed (Fig. 5d and 6). As a result, the blurry ^{82}Se signal is likely due to matrix interference and not a sign of quantum dot degradation despite the poor r values found in Table 3.

It is worth noting that an unusual ^{63}Cu summit appears opposite to the ^{114}Cd hot zones (Fig. 6). Element distribution images of control experiments are shown in Fig. 7. From Fig. 7, the distribution of ^{31}P, ^{66}Zn, and ^{56}Fe seems unaffected by the presence of quantum dots. However, the distribution of ^{63}Cu showed quite different pattern where no significant hot zones were observed. This means that the distribution of ^{63}Cu is rather homogeneous without treatment of quantum dots. The monitored essential elements (^{63}Cu, ^{31}P, and ^{66}Zn) have comparable patterns in the spleen, liver and other organs (muscle, brain, and lung, data not shown). In the kidney, comparable intensity profiles are seen for ^{31}P and ^{66}Zn while there is a markedly different distribution of ^{63}Cu. This is likely due to certain biointereactions between the kidney and the quantum dots. The most famous cases regarding the abnormal distribution of copper in the kidney are Wilson disease and Menkes disease. In a murine model, the inactivation of Cu-ATPase caused by Wilson disease or Menkes disease results in significant copper accumulation in the kidneys, particularly in proximal tubules of the cortex [25]. The mice used in this study did not suffer from either of these diseases (with certification from BioLASCO) as both are genetic diseases. Identification of what kind of biointeraction is taking place requires a more specific technique such as an immunolocalization technique. However, it is clear that LA-ICP-MS is capable of revealing the biointeractions between quantum dots and in vivo tissues, which is quite difficult to accomplish with conventional ICP-MS system and fluorescence spectrometry.

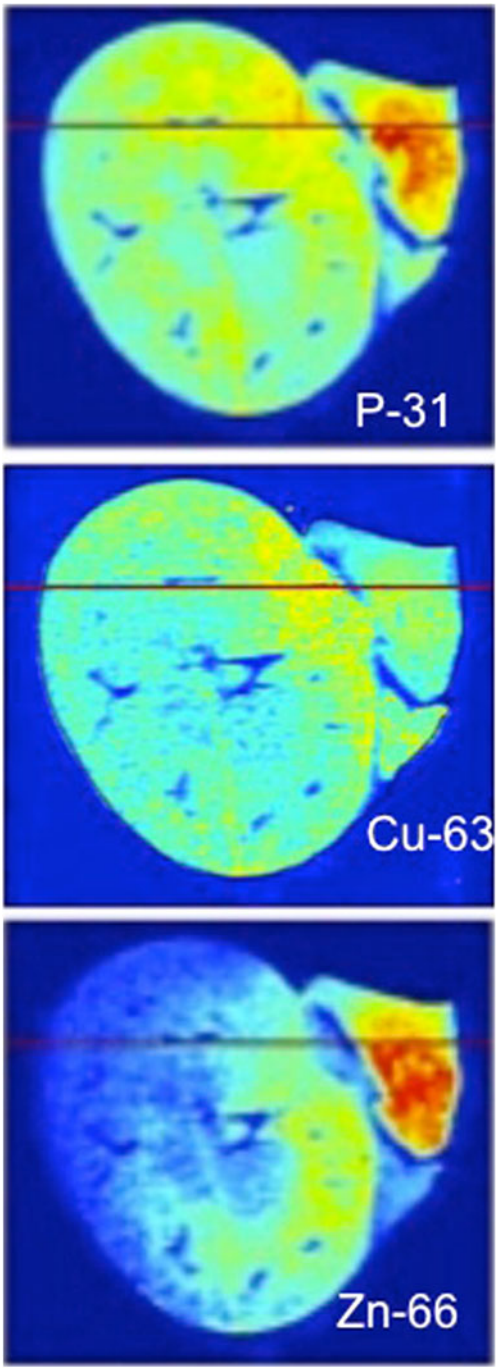

Fig. 7 The distribution images of ^{31}P, ^{63}Cu, and ^{66}Zn in the kidney of control experiments; the region with *red color* is the location of high intensity while the one in *blue* means very low intensity. While the distribution of ^{31}P and ^{66}Zn seems unaffected by the introduction of quantum dots, it is obvious that no particular ^{63}Cu hot zones were noticed

Conclusion

LA-ICP-MS displays significant advantages in spatial resolution from the laser ablation component and multielement

analysis from the ICP-MS detector. These advantages illustrate that LA-ICP-MS is a powerful tool to probe the fate and biodistribution of quantum dots in vivo. In this study, it was observed that, in the murine model, quantum dots administrated by intravenous injection mainly accumulated in the red pulps of the spleen, portal areas of the liver and adrenal glands of the kidney within 1 h. It is believed that the quantum dots have not degraded as evidenced by the intensity of the fluorescence in the fluorescence spectrum image and comparable intensity profile of ^{114}Cd and ^{82}Se, despite the slight probability for a statistical point of view. While, there was no evidence supporting cytotoxicity of quantum dots in the spleen and the liver, there was an obvious immune response involving abnormal copper distribution in the kidney. Based on the results presented here, it is not possible to determine the kind of immune reaction and the cytotoxicity associated with the reaction. However, the results illustrate the usefulness of LA-ICP-MS in determining the presence and distribution of various elements in tissues.

Acknowledgements This work was supported by the National Science Council, Taiwan under grant NSC-100-2221-E-007-012. We gratefully acknowledge Mr. WenFeng Chang for the LA-ICP-MS measurement and Mr. Camden Henderson for English correction.

References

1. Lee S-HA, Zhao YX, Hernandez-Pagan EA, Blasdel L, Youngblood WJ, Mallouk TE (2012) Electron transfer kinetics in water splitting dye-sensitized solar cells based on core-shell oxide electrodes. Faraday Discuss 2012(155):165–176
2. Zhao YX, Vargas-Barbosa NM, Hernandez-Pagan EA, Mallouk TE (2011) Anodic deposition of colloidal iridium oxide thin films from hexahydroxyiridate(IV) solutions. Small 2011(7):2087–2093
3. Cassagneau T, Mallouk TE, Fendler J (1998) Heterosupramolecular assembly of zener diodes from conducting polymers and CdSe nanoparticles. J Am Chem Soc 1998(120):7848–7859
4. Youngblood WJ, Lee SHA, Maeda K, Mallouk TE (2009) Visible light water splitting using dye-sensitized oxide semiconductors. Acc Chem Res 2009(42):1966–1972
5. Guo X, Wang CF, Yu ZY, Chen L, Chen S (2012) Facile access to versatile fluorescent carbon dots toward light-emitting diodes. Chem Comm 2012(48):2692–2694
6. Jacobsson TJ, Edvinsson T (2011) Absorption and fluorescence spectroscopy of growing ZnO quantum dots: size and band gap correlation and evidence of mobile trap states. Inorg Chem 2011 (50):9578–9586
7. Srivastava BB, Jana S, Pradhan N (2011) Doping Cu in semiconductor nanocrystals: some old and some new physical insights. J Am Chem Soc 2011(133):1007–1015
8. Wu CF, Schneider T, Zeigler M, Yu JB, Schiro PG, Burnham DR, McNeill JD, Chiu DT (2010) Bioconjugation of ultrabright semiconducting polymer dots for specific cellular targeting. J Am Chem Soc 2010(132):15410–15417
9. Bouzigues C, Gacoin T, Alexandrou A (2011) Biological applications of rare-earth based nanoparticles. ACS Nano 2011(5):8488–8505
10. Depalo N, Carrieri P, Comparelli R, Striccoli M, Agostiano A, Bertinetti L, Innocenti C, Sangregorio C, Curri ML (2011) Biofunctionalization of anisotropic nanocrystalline semiconductor-magnetic heterostructures. Langmuir 2011(27):6962–6970
11. Song EQ, Hu J, Wen CY, Tian ZQ, Yu X, Zhang ZL, Shi YB, Pang DW (2011) Fluorescent-magnetic-biotargeting multifunctional nanobioprobes for detecting and isolating multiple types of tumor cells. ACS Nano 2011(5):761–770
12. Huang XL, Li LL, Liu TL, Hao NJ, Liu HY, Chen D, Tang FQ (2011) The shape effect of mesoporous silica nanoparticles on biodistribution, clearance, and biocompatibility in vivo. ACS Nano 2011(5):5390–5399
13. Derfus AM, Chan WCW, Bhatia SN (2004) Probing the cytotoxicity of semiconductor quantum dots. Nano Lett 2004(4):11–18
14. Yildirimer L, Thanh NTK, Loizidou M, Seifalian AM (2011) Toxicological considerations of clinically applicable nanoparticles. Nano Today 2011(6):585–607
15. Sato K, Yokosuka S, Takigami Y, Hirakuri K, Fujioka K, Manome Y, Sukegawa H, Iwai H, Fukata N (2011) Size-tunable silicon/iron oxide hybrid nanoparticles with fluorescence, superparamagnetism, and biocompatibility. J Am Chem Soc 2011(133):18626–18633
16. Liu Q, Sun Y, Yang TS, Feng W, Li CG, Li FY (2011) Sub-10 nm hexagonal lanthanide-doped NaLuF(4) upconversion nanocrystals for sensitive bioimaging in vivo. J Am Chem Soc 2011(133):17122–17125
17. Tan A, Yildirimer L, Rajadas J, De La Pena H, Pastorin G, Seifalian A (2011) Quantum dots and carbon nanotubes in oncology: a review on emerging theranostic applications in nanomedicine. Nanomedicine 2011(6):1101–1114
18. Rojas S, Gispert JD, Martin R, Abad S, Menchon C, Pareto D, Victor VM, Alvaro M, Garcia H, Herance JR (2011) Biodistribution of amino-functionalized diamond nanoparticles. In vivo studies based on (18)F radionuclide emission. ACS Nano 2011 (5):5552–5559
19. Moore KL, Lombi E, Zhao FJ, Grovenor CRM (2012) Elemental imaging at the nanoscale: NanoSIMS and complementary techniques for element localization in plants. Anal Bioanal Chem 2012 (402):3263–3273
20. Akahoshi N, Ishizaki I, Naya M, Maekawa T, Yamazoe S, Horiuchi T, Kajimura M, Ohashi Y, Suematsu M, Ishii I (2012) TOF-SIMS imaging of halide/thiocyanate anions and hydrogen sulfide in mouse kidney sections using silver-deposited plates. Anal Bioanal Chem 2012(402):1859–1864
21. Wu B, Becker JS (2011) Imaging of elements and molecules in biological tissues and cells in the low-micrometer and nanometer range. Int J Mass Spectrom 2012(307):112–122
22. Su CK, Huang CW, Yang CS, Wang YJ, Sun YC (2010) In vivo monitoring of quantum dots in the extracellular space using push–pull perfusion sampling, online in-tube solid phase extraction, and inductively coupled plasma mass spectrometry. Anal Chem 2010 (82):7096–7102
23. Zhu ZJ, Ghosh PS, Miranda OR, Vachat RW, Rotello VM (2008) Multiplexed screening of cellular uptake of gold nanoparticles using laser desorption/ionization mass spectrometry. J Am Chem Soc 2008(130):14139–14143
24. Zhu ZJ, Tang R, Yeh YC, Miranda OR, Rotello VM, Vachat RW (2012) Determination of intracellular stability of gold nanoparticle monolayers using mass spectrometry. Anal Chem 2012(184):4321–4326

25. Lutsenko S, Barnes NL, Bartee MY, Dmitriev OY (2007) Function and regulation of human copper-transporting ATPases. Physiol Rev 2007(87):1011–1046
26. Becker J, Gorbunoff A, Zoriy M, Izmer A, Kayser M (2006) Evidence of near-field laser ablation inductively coupled plasma mass spectrometry (NF-LA-ICP-MS) at nanometre scale for elemental and isotopic analysis on gels and biological samples. J Anal At Spectrom 21:19–25
27. Zhu ZJ, Yeh YC, Tang R, Yan B, Tamayo J, Vachet RW, Rotello VM (2011) Stability of quantum dots in live cells. Nat Chem 2011 (3):963–968
28. Navarro DA, Banerjee S, Watson DF, Aga DS (2011) Differences in soil mobility and degradability between water-dispersible CdSe and CdSe/ZnS quantum dots. Environ Sci Technol 2011 (15):6343–6349